Environmentally-stable eco-friendly pectin-silica bio-hybrid foams for soil remediation

Sarah Christoph, Pierre Barré, Bernard Haye, Thibaud Coradin, Francisco M. Fernandes

Giant, 12, 2022, 100119

Full-length article

Environmentally-stable eco-friendly pectin-silica bio-hybrid foams for soil remediation

Sarah Christoph[a], **Pierre Barré**[b], **Bernard Haye**[a], **Thibaud Coradin**[a,*], **Francisco M. Fernandes**[a,*]

[a] Sorbonne Université, CNRS, Chimie de la Matière Condensée de Paris, Paris F-75005, France
[b] PSL University, CNRS, Laboratoire de Géologie, Ecole Normale Supérieure, Paris F-75231, France

Keywords: Hybrid materials, Pectin, Silica, Ice-templating, Soil remediation

Here we present a new class of hybrid material composed of a polysaccharide macroporous core surrounded by a thin silica layer as new adsorption platforms for the retention of organic pollutants in soil media. The core-shell hybrid foams were fabricated by ice-templating to create highly anisotropic pectin foams, followed by vapor phase silica deposition. The structural stability of the hybrid foams was tested in compression, reaching a Young's Modulus up to 5 MPa, but also, and more importantly, in direct contact with wet soils over more than one month. Hybrid foams showed a sorption capacity for a toxic dye nearly two orders of magnitude higher than the surrounding soils. Altogether, these hybrid foams combine all chemical, structural and functional properties required to be effective materials for soil depollution and, thanks to their easy-recovery, should compete with common particulate sorbents.

1 Introduction

Soil encompasses representatives of all biological kingdoms, making it a centerpiece of most ecosystems [1]. Loss of soil quality, through physical or chemical degradation, results in a wide range of negative consequences that can endanger the local fauna and flora, and threaten human health indirectly through different pathways including food and water consumption [2–4]. What is commonly referred to as soil pollution is the addition of exogenous -potentially toxic-compounds that may enter organisms through transfer in another medium (air or water) [5]. Therefore, one key approach to limit risks associated with pollution is to immobilize the compounds within the soil, limiting their bioavailability [6]. Techniques such as stabilization/solidification [7] or capping [8] are designed to limit the mobility of the pollutants. These approaches have however the drawback of leaving the pollutant within the soil, which may be problematic in the long run, since soils may undergo significant physical and chemical modifications [9]. Pollutants may also be physically removed from the polluted sites. The most straightforward approach is excavation, which is usually combined with other techniques such as thermal desorption [10] or soil washing [11]. These methods are usually complex from a logistical point of view, especially in the case of large contaminated areas [9].

It is also possible to treat contaminated soil thanks to *in situ* methods. *In situ* thermal treatment allows for extraction of the contaminant without excavation and in some case for direct degradation of the targeted chemicals [12]. The recovered contaminants must then be stored or treated appropriately.

* Corresponding authors.
E-mail addresses: thibaud.coradin@sorbonne-universite.fr (T. Coradin), francisco.fernandes@sorbonne-universite.fr (F.M. Fernandes).
Received 27 June 2022; Received in revised form 13 September 2022; Accepted 7 October 2022

https://doi.org/10.1016/j.giant.2022.100119

Pollutants may also be degraded directly within the soil using for instance oxidation [13]. This however requires addition of oxidizing or reducing chemicals to the contaminated sites. Today, the most promising alternative to these physical and chemical techniques is to take advantage of the removal and/or degradation capabilities displayed by a wide variety of living organisms but with a risk of dissemination of exogeneous organisms [14–16].

Similarly to water decontamination, solid adsorbents may constitute a cost-effective and easy-to-implement solution to manage the bioavailability of pollutants in soils [17]. As for water treatment, constituting materials must be chemically stable, mechanically-robust and prepared from non-toxic constituents [18]. However, the two kinds of environments differ in several important aspects, that strongly impact the remediation process [19]. First soils are usually highly adsorbing media so that the removal capacity of the material should be very high to displace the pollutants [20]. Second, whereas micro- and nano-particles exhibiting high specific surface area and high sorption capacity, such as clays and biochars [21,22], can be used in liquid media because they can be easily recovered, materials used in soils must be large enough to be easily collected.

Taking all these constraints in charge, we hypothesized that a macroscale material with oriented macroporosity -to favor water uptake by capillary effects- would be particularly well-suited. Ice-templating (also referred to as freeze-casting) is a technique initially developed to shape lightweight ceramic materials [23] that has been applied to composite, metallic and (bio)polymer-based materials [24–26]. The technique allows for a straightforward control over the macroporosity of the prepared materials, which led to an increasing popularity in a myriad of applications [27], ranging from biomaterials [28,29] to energy [30,31] and sensing [32,33]. As constituents, we focused on pectin as an abundant biomacromolecule of vegetal origin, being therefore fully compatible with the soil biota [34]. In order to stabilize the pectin network, we have used a vapor phase coating strategy, derived from the Biosil process [35], to deposit silica, the major mineral phase of many soils exhibiting therefore no environmental impact [36]. We demonstrate that optimization of ice templating and mineral deposition conditions, it is possible to obtain pectin-silica foams with improved mechanical properties and water stability. Moreover, we offer the first experimental evidence that such bio-hybrid foams are stable in soils over one month and exhibit the ability to efficiently immobilize a toxic dye in such environments.

2 Materials and methods

2.1 Hybrid pectin foams

Macroporous pectin foams were obtained by freeze-casting 3 mL samples of 4 wt% sugar beet pectin suspension in PIPES buffer at 1, 5 and 10 °C.min^{-1} and subsequent lyophilization [37]. Foams were maintained in a desiccated atmosphere until further use. For the vapor phase silica deposition, dry samples were placed in a closed vessel (approximate volume 1 L) containing a solution composed of 133 mL of deionized water, 17 mL of 37% HCl and 60 g of NaCl. Four vials ($Ø$ = 29 mm) containing 10 mL of tetraethyl orthosilicate (TEOS) each were also placed within the vessel. The setup was maintained at 30 °C (up to two weeks) depending on the desired silica content. Samples were then dried 24 h at 30 °C and kept at room temperature under desiccated atmosphere.

Scanning Electron Microscopy (SEM) observation was carried out on Hitachi S-3400 N after cutting of the samples and sputtering with a 20 nm layer of Gold. SEM-FEG observation was carried out on Hitachi SU-70 equipped with a Field Emission Gun after cutting of the samples and sputtering with a 5 nm Platinum layer. Pore morphology characterization was performed using the Orientation J plugin in FIJI software [37].

Mechanical testing was performed in compression under an Instron 5965 universal testing machine at 1 mm.min^{-1} crosshead speed up to 50% strain. Core-shell hybrid foams were prepared as previously described into 5 × 5 × 5 mm^3 samples.

2.2 Foam stability in soils

Each sample (*ca*. 40 mg) was placed in 110 g of soil rehydrated by 18 mL of deionized water (corresponding to pF 2.5, optimal humidity conditions for the soil microbial community). The chosen reference soil was upper horizon of a silt loam Luvisol sampled at the Versailles INRA station, France. The chosen upper horizon (Ap) was composed of 18% clay, 57% silt and 25% sand. The soil's cation exchange capacity was equal to 11 cmol(+) kg^{-1} and was mainly saturated by calcium. Its pH was equal to 6.1 and the total organic C content of the upper horizon 13 g C/kg soil. The vials were sealed with Parafilm^{TM} to prevent soil desiccation and maintained at 20 °C in the dark. Freeze dried pectin foams were used as controls and compared to pectin foams coated with silica through exposition to TEOS vapors. Silica contents ranged from 0% SiO_2 to 39% SiO_2. After incubation in soil, foam samples were removed after 1, 6, 20 and 37 days and dehydrated in successive baths of increasing ethanol content (20, 40, 60, 80 and 100%) for SEM observation.

2.3 Dye immobilization experiments

For these experiments, individual hybrid foams (40 mg, 39% SiO_2) were covered with 10 g of soil saturated with 7 mL of a 100 mg.L^{-1} aqueous solution of Reactive Black 5. In parallel, the same amount of soil was exposed to 7 mL of a 100 mg.L^{-1} aqueous solution of Reactive Black 5 in the absence of hybrid foams. The soil was incubated for 24 h at 25 °C. After washing with 7 mL PBS 2X to simulate water infiltration, the supernatant was centrifuged for 10 min at 5000 rpm and absorbance at 598 nm was measured to calculate the remaining Reactive Black 5 concentration. Control sample consisted of the dye solution at the start of the experiment (t = 0) and after 24 h of incubation at 25 °C (t = 24)

3 Results and discussion

3.1 Design of biopolymer-silica macroporous foams

Hybrid foams were prepared by applying ice templating to a beetroot pectin solution followed by silica deposition through exposure to vapors of silica precursor (TEOS) under acidic atmosphere (Fig. 1)

Based on previous results [37], pectin concentration was fixed to 4 wt% and the freezing rate was varied between 1 and 10 °C.min^{-1}. As shown on Fig. 2a–f, the materials are characterized by a lamellar structure, where the elongated pores are organized in

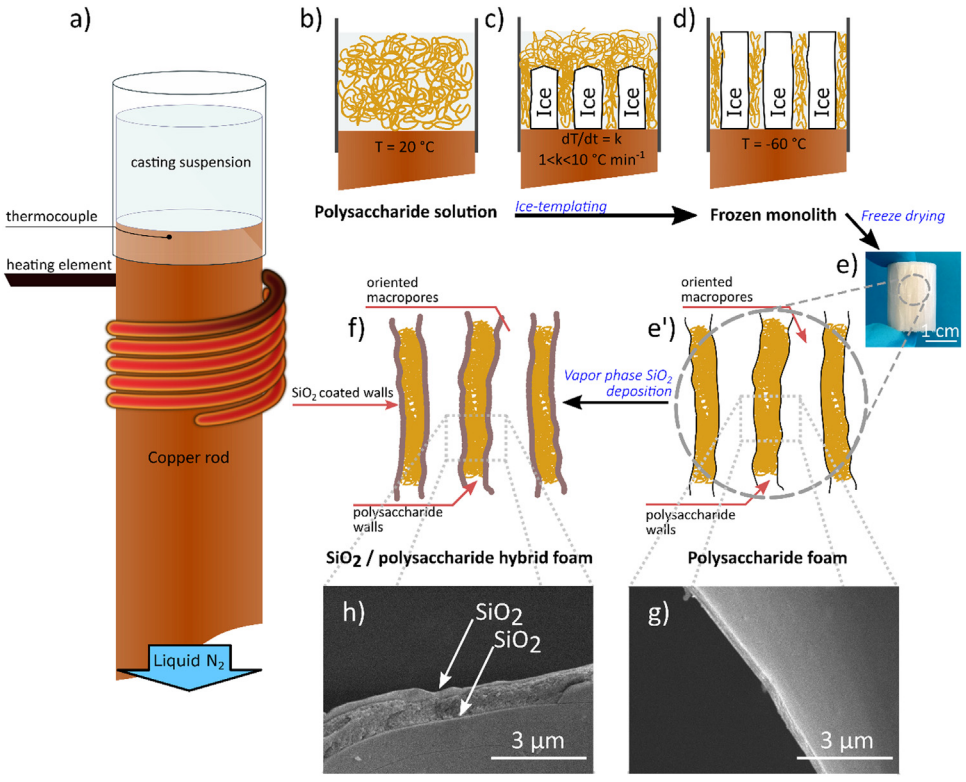

Fig. 1

Overview of the fabrication process of pectin-silica foams. (a) Simplified scheme of the ice templating setup used to shape the macroporous monoliths, (b–d) Ice templating processing steps leading to the formation of a frozen monolith. (e,e') Lyophilization yields a solid polysaccharide foam. Scanning electron micrographs of the polysaccharide foams (g) before and (h) after silica coating under tetraethoxysilane vapors.

several domains of same orientation. Analysis of SEM pictures of cross sections reveal slight pore size variations with cooling rate. Mean pore length varies from 428 µm to 309 µm when the cooling rate increases (Fig. 2g). The large standard deviations for these values must however be underlined. This may be explained by the length variations observed in each orientation domain. A more significant parameter to describe the cellular material morphology is the pore width, which present smaller deviations (Fig. 2h). The pores' mean width ranged from 10.4 µm at 10 °C.min^{-1} to 18.7 µm at 1 °C.min^{-1}. Slower freezing favors ice crystal growth, resulting in larger ice crystals and, consequently in larger pores after freeze drying [38]. A decrease in the pore wall width can also be observed at higher cooling rates (200 nm at 10 °C.min^{-1} vs 312 nm at 1 °C.min^{-1}) (Fig. 2i). Because all samples have equal apparent density, increasing the number of pores per section area (i.e. when pores are smaller) results in decreased pore wall thickness due to reduced amount of polymer available for each wall.

The orientation analysis of the pores (Fig. 3) allows to describe the inner structure of the macroporous materials in more detail. Regardless of the cooling rate, several orientation domains can be observed on SEM images of the foams' cross sections, as depicted in the angular distribution of the pores' cross-sectional main axis (Fig. 3a'–c') which correspond to the different lamellar domains. On the contrary, the analysis of the pores' orientation in the longitudinal sections of the foams (cut along the ice growth direction) do not display any noticeable dependence with the cooling rate (Fig. 3d'–f').

These slight structural changes have no clear influence on the mechanical properties of the foams. Values for Young's modulus and compressive strength of foams obtained at different freezing rates are presented in Supplementary Fig. S1. Young's modulus values are around 3 MPa and compressive strengths are about 0.1 MPa which are typical values for flexible polymer foams [39]. The wetting behavior of the foams was also studied by surface impregnation with an ethanolic solution containing the Disperse Red 1 dye. Full wetting was achieved within less than one second, with no significant variation with freezing rate (Supplementary Fig. S2). Altogether, freezing rate had little if any influence on the macroscopic properties of the foams. The highest freezing rate was therefore selected for the following study, both because it leads to the smaller average pore size that could enhance capillary effects, but also as it allows for faster preparation of the foams.

However, it was found that pectin foams rapidly (*i.e.* < 1 day) redisperse in water, as expected from the physical nature of pectin hydrogels (Supplementary Fig. S3). To address this issue, cross-linking did not appear as a viable option as it would require placing the unstable foam in an aqueous environment and/or using potentially toxic additives [40]. As an alternative, we used a gas phase deposition process inspired by the Biosil technology

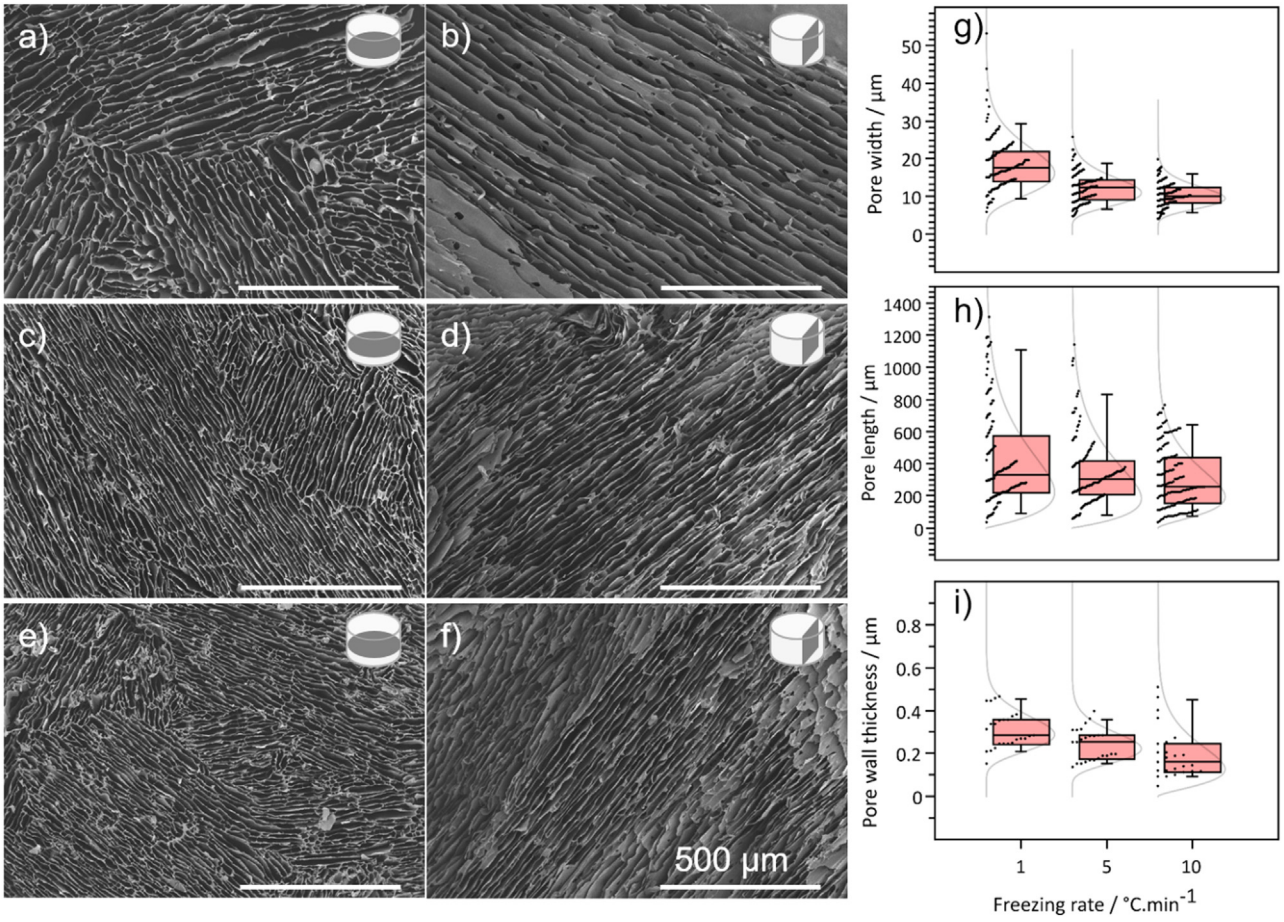

Fig. 2

SEM imaging and pore morphology characterization of pectin foams. (a-f) SEM images of the pectin foams along (left-hand column) and perpendicular (right-hand column) to the freezing direction at a) 1, b) 5 and c) 10 °C.min^{-1} All scale bars correspond to 500 µm. (g) pore width, (h) pore length and (i) pore wall thickness distributions as obtained using SEM image analysis on ImageJ.

[35] to coat the pore wall with amorphous silica, a fully eco-friendly mineral phase [36].

With this purpose, dry foams were placed in a closed vessel in the presence of TEOS, water and HCl vapors for up to 14 days. FT-IR spectroscopy was used as a simple method to check the chemical nature of the deposited phase. The typical peaks of hydrated silica around $\nu^{a}_{Si\text{-}O}$ = 1070 cm^{-1}, $\nu^{s}_{Si\text{-}O\text{-}Si}$ = 800 cm^{-1} and $\nu_{Si\text{-}OH}$ = 930–950 cm^{-1} could be evidenced [41], that grew in intensity with deposition time (Supplementary Fig. S4). The most direct way to quantify the presence of silica after contact with vapors of TEOS was to weight the samples before and after the treatment. Sample weight increases between 0.3 mg and 60 mg in a 15 days-time span, which correspond to weight percentages between 0.5%$_{SiO2}$ and 46%$_{SiO2}$. (Fig. 4(g)). Mass gain was important during the first few days, but reaches a plateau after longer expositions (after about one week). Such phenomenon should sign for the saturation of pore surface coverage.

SEM imaging allowed to estimate the coating thickness that reach more than 100 nm (Fig. 4a–f**)**. However, while up to *ca*. 40 wt% silica content, the standard deviation was reasonably low, much more variability was observed for higher SiO_2 content due to more heterogeneous coatings (Fig. 4h). This can be linked to the kinetic data of deposition showing that such a 40 wt% silica content is a limit value above which weight variations become less regular.

The effect of silica addition on the stabilization of the foam against dissolution in water was checked by soaking the samples in water. At 37%$_{SiO2}$, the hybrid material retains its integrity up to 3 weeks (Supplementary Fig. S3) suggesting this weight fraction corresponds to a percolating layer covering the entirety of the foam surfaces -both internal and external. Silica was added to the pectin foams primarily to ensure protection against dissolution of the structure. However, addition of the inorganic material to the polymer foam was expected to modify other properties of the material, in particular its mechanical response to compression, a key parameter to ensure the stability of lightweight materials in compressive media such as soils. Fig. 5 presents the stress/strain curves as well as Young's moduli, toughness and yield strength depending on the silica content. Up to about 20%$_{SiO2}$ the mechanical properties of the material appear similar to those of the pectin alone. SEM observations suggested that the corresponding coating was not continuous, *i.e*. the deposited

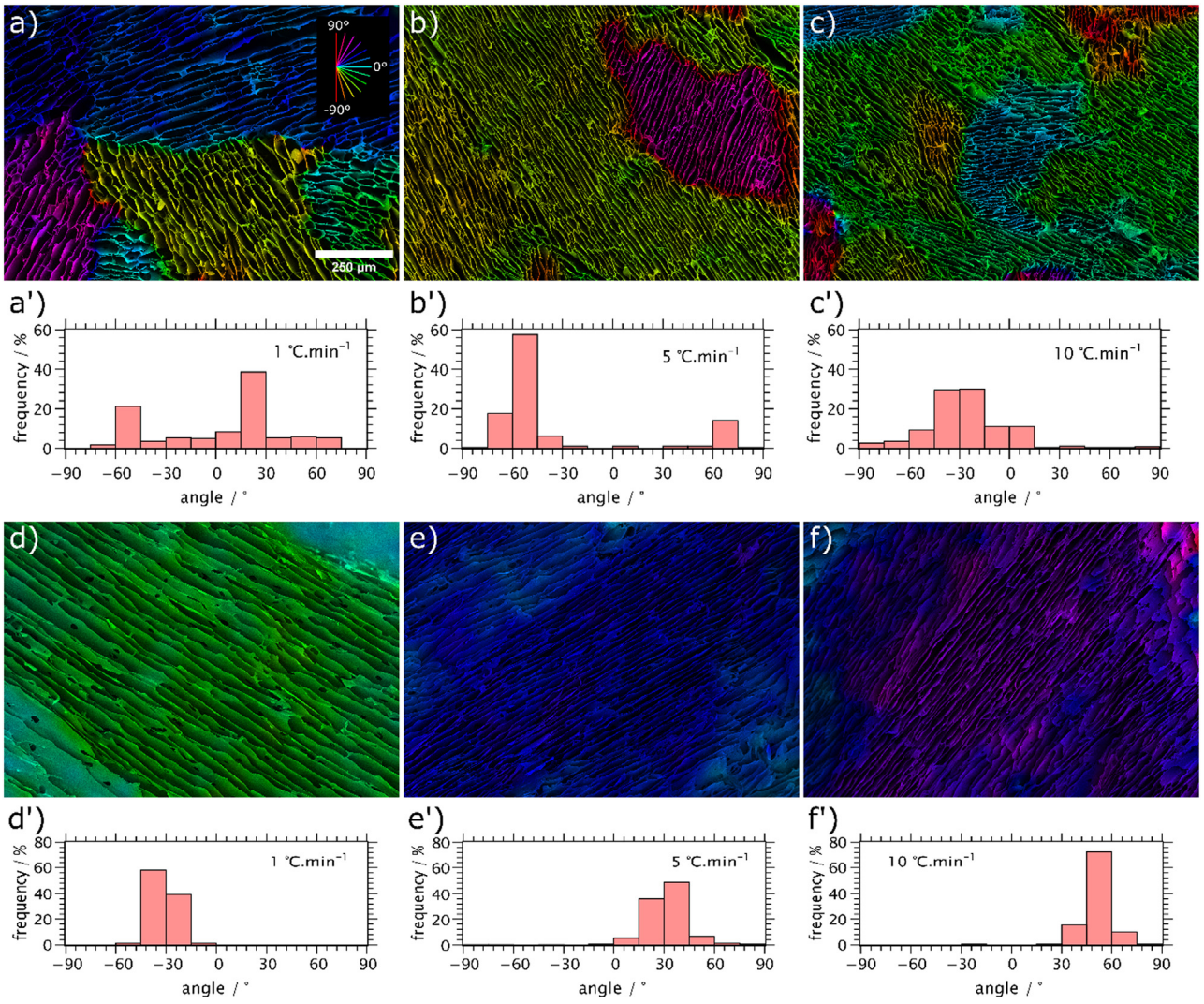

Fig. 3

Directional analysis of pectin foams' pores obtained at different cooling rates. SEM images of the cross-section of pectin foams (image taken along the freezing direction) at 1 (a), 5 (b) and 10 °C.min^{-1} (c) treated using OrientationJ plugin in FIJI and respective pore orientation histograms (a' to c'). SEM images of the pectin foams perpendicular to the freezing direction at 1 (d), 5 (e) and 10 °C.min^{-1} f) treated using OrientationJ plugin in FIJI and respective pore orientation histograms (d' to f'). Scale bar for all images is 250 µm.

silica particles density was below a percolating threshold. This scattered deposition could configure a sparse distribution of silica-rich areas on the surface of the foams, with minimal impact over the materials' elastic properties. Above this value, higher mass percentages of the inorganic moiety result in stiffer inorganic material, with higher toughness and yield strength. These values are in good agreement with the enhanced water stability for 37%$_{SiO2}$ as discussed above.

3.2 Foam behavior in soils

In soils, materials are exposed to several physico-chemical factors such as pH, temperature, humidity, as well as to a myriad of organic and inorganic compounds ranging from complex polysaccharides to sand and clays. In addition, materials in soils are exposed to endogenous micro-organisms, which may induce substantial degradation.

To ascertain the stability of the synthesized materials towards such conditions, both pectin silica-coated pectin samples were introduced into real soils, conditioned at constant humidity and temperature. Importantly, the soils were not sterilized, meaning that the prepared materials were directly brought into contact with the soil's microbiota (bacteria, yeast, fungi, etc.). Samples were dug out at various time points to assess their integrity.

Fig. 6(a) shows the aspect -at the micro- and macroscopic length-scales- of pectin-based foams after up to 1 month of exposure to the reference soil (upper horizon (0–30 cm) of a silt loam Luvisol sampled at the Versailles INRAE station). After only 24 h the pectin foams (with no silica) appear severely deteriorated, which is likely to be mostly due to the dissolution of the pectin structure upon exposure to the moisture of the soil. The addition of a silica coating seems efficient in preventing

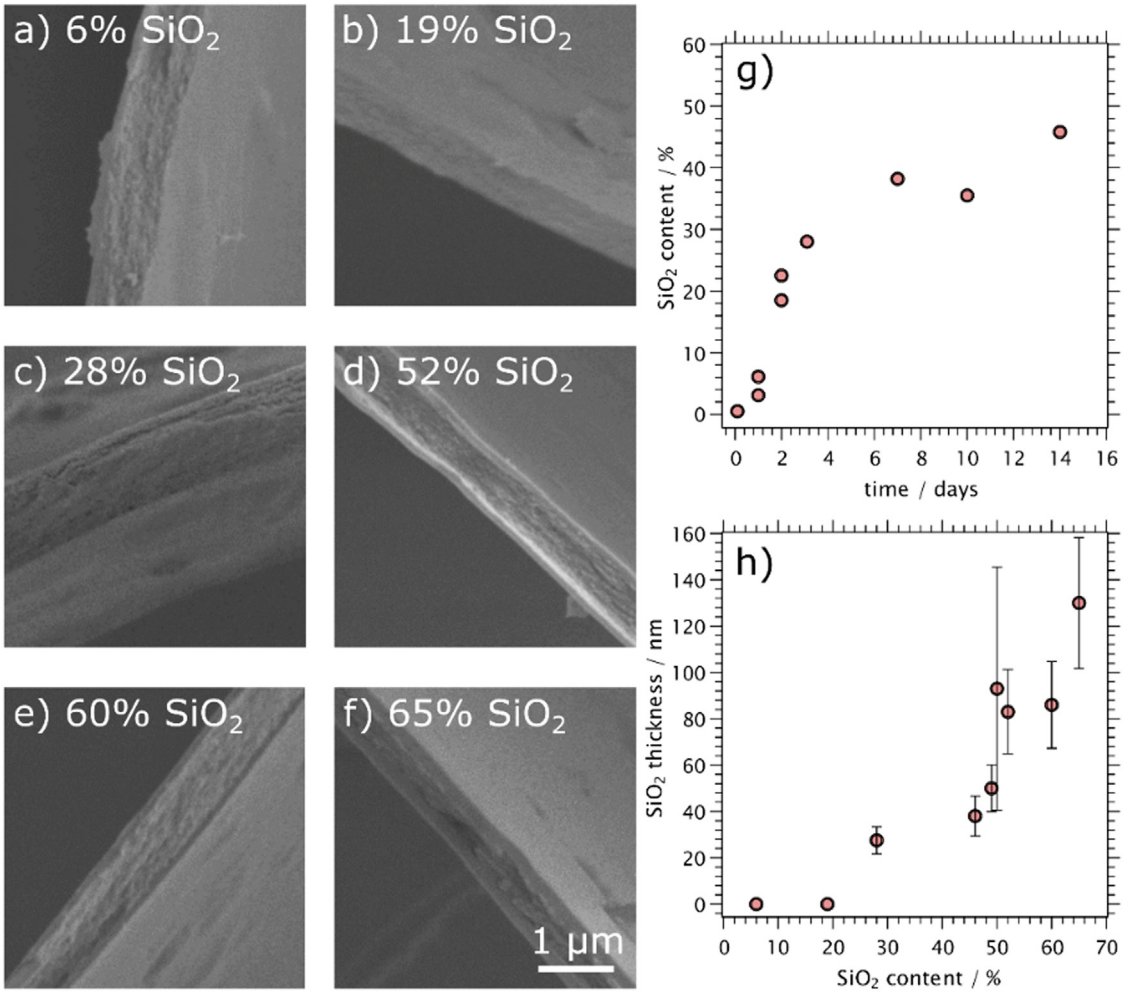

Fig. 4

Characterization of silica deposition in hybrid foams. (a-f) SEM images of the pectin walls covered by increasing silica contents. (g) Variation of silica content with deposition time. (h) Variation of silica shell thickness with silica content.

immediate dissolution of the pectin foams. Degradation of foams containing low amounts of silica was delayed, however after 20 days the samples undergo significant deterioration. Such degradation is probably due to a combination of microbial activity from the non-sterile soil and partial dissolution of the pectin pore walls due to incomplete percolation of the silica layer. Higher silica content may be associated with the formation of a fully percolated silica coating. It results in enhanced stability of the samples, which appear unaltered after one month in the model soil. In parallel with the macroscopic assessment of the foams' integrity, their microscopic structure was assessed by SEM observation after drying. Quantitative measurements of the SEM images were conducted based on image coherency measurements [42]. Isotropic images yield low coherency values (close to zero) and highly anisotropic images yield higher values (close to one). Here, coherency values calculated from the entire SEM insets displayed in Fig. 6a were analyzed using the Orientation J plugin on FIJI and are displayed in Fig. 6b. The coherency values obtained confirm the maintenance of the highly aligned structures at higher SiO_2 contents, whereas SiO_2 mass fractions below 25 wt% do not prevent the loss of the sample's aligned structures. The addition of silica seems efficient in preserving the oriented macroporous structure, especially at high silica content, both at the macro- and microscopic scales.

Finally, we performed a preliminary evaluation of the ability of foams to efficiently adsorb organic contaminants when placed within soils. To point out the efficiency of the sorbent, the foam over soil weight ratio was kept below 1 wt%. The Reactive Black 5 dye was selected due to its high toxicity and difficulty to be removed from soils [43]. As seen on Fig. 7, the dye solution underwent noticeable discoloration in the presence of the soil alone and showed only a faint color when the foam was present. Quantification by monitoring the UV–vis spectra of the supernatant indicates that while the soil alone immobilized *ca.* 60% of the dye, this amount reaches more than 80% with the foam. Considering the initial foam/soil weight ratio (<1%), it means that the apparent sorption capacity of the macroporous material is *ca.* 50 times larger than that of its environment. Such a high difference in fact suggests that the foam is able to displace dyes from the soil particles.

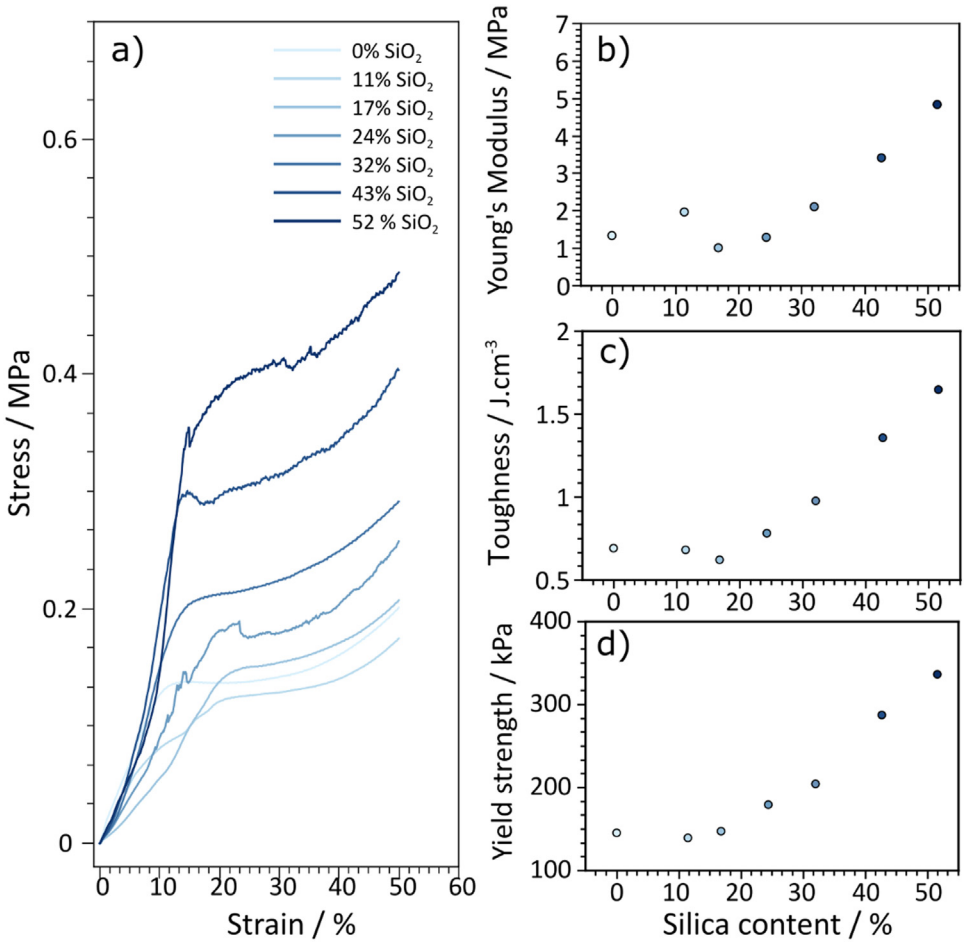

Fig. 5

Mechanical properties of hybrid pectin-silica foams. (a) Stress-strain profiles of pectin core/silica shell hybrid foams. (b-d) Young's modulus, toughness, and yield strength according to the silica composition. Due to the variability inherent to the silica deposition process only one sample has been produced per silica content condition except for the 0% SiO_2 ($n = 5$).

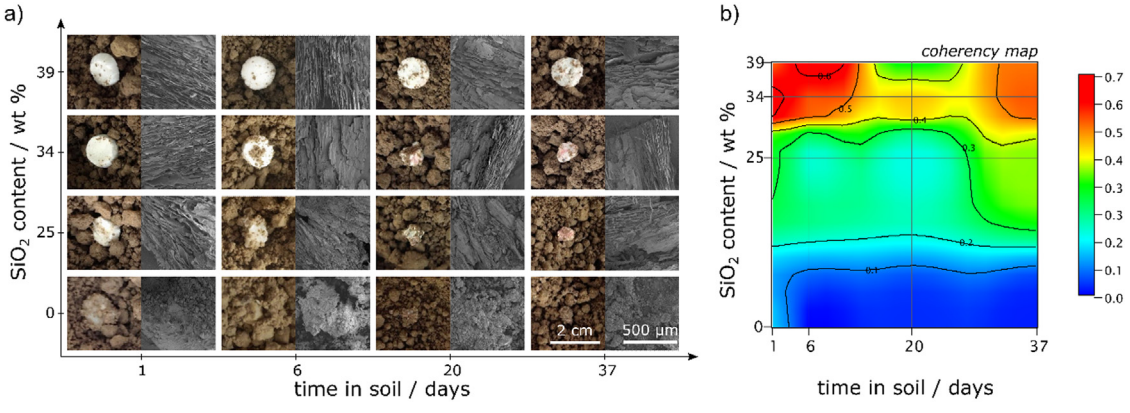

Fig. 6

Evolution of pure and hybrid pectin foams with increasing SiO_2 content when placed in upper horizon of silt loam Luvisol soil. (a) For each SiO_2 composition and each timepoint two images are presented: on the left, macroscopic images of samples after recovery from soil, and on the right, SEM images of the same samples. Soils were conditioned at controlled moisture conditions (field capacity, pF = 2.5) and temperature (20 °C). (b) Coherency map calculated from SEM images presents in (a).

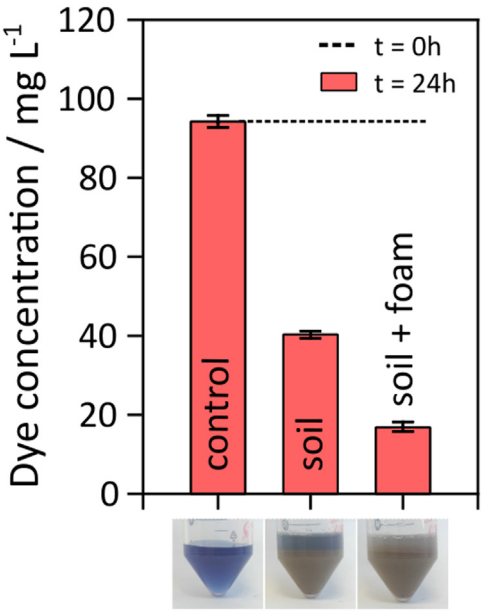

Fig. 7

Dye adsorption experiments. Dye concentration after 24 h as such (control) or in contact with soil or foam in soil. Lower row depicts, from left to right, the dye solution, the dye solution in contact with soil, and the dye solution after being in contact with a foam inside the soil.

4 Conclusion

By combining two environmentally-friendly components, pectin and silica, and using easy-to-implement technologies, freeze-casting and vapor phase deposition, it was possible to obtain materials that are stable in soils and show the ability to displace and immobilize a highly toxic organic dye. Importantly, compared to other possible soil-compatible microscale sorbents, such as clays, they are efficient as macroscale materials, allowing for their easy recovery. This can be attributed to their oriented porosity that compensates the decrease in surface area by favoring contact between contaminated running waters and sorbing surfaces via capillary effects. A more systematic investigation of the influence of pore geometry and dimension should allow to enhance this effect further. Meanwhile functionalization of the silica layer by natural organic, inorganic or even biological species with sorbing/degrading capabilities can be envisioned.

Funding sources

This work was funded by the French Ministry of Superior Education and Research (Ecole Doctorale 397) and supported by the Investissements d'Avenir programme [ANR-11-IDEX-0004–02], and more specifically within the framework of the Cluster of Excellence MATISSE led by Sorbonne Universités. This source had no involvement in work conduction and manuscript submission.

Declaration of Competing Interest

The authors declare that they have no known competing financial interests or personal relationships that could have appeared to influence the work reported in this paper.

Data Availability

Data will be made available on request.

CRediT authorship contribution statement

Sarah Christoph: Methodology, Formal analysis, Investigation, Writing – original draft, Visualization, Funding acquisition. **Pierre Barré:** Methodology, Validation, Resources, Writing – review & editing. **Bernard Haye:** Investigation. **Thibaud Coradin:** Conceptualization, Validation, Writing – original draft, Supervision, Project administration, Funding acquisition. **Francisco M. Fernandes:** Conceptualization, Methodology, Validation, Formal analysis, Writing – original draft, Visualization, Supervision, Funding acquisition.

Acknowledgments

The authors would like to acknowledge G. Mosser and P. Le Griel (LCMCP) for TEM imaging

Supplementary materials

Supplementary material associated with this article can be found, in the online version, at doi:10.1016/j.giant.2022.100119.

References

[1] F. Carvalho Nunes, L. de Jesus Alves, C.C. Nolasco de Carvalho, E. Gross, T. de Marchi Soares, M.N.V. Prasad, M.N.V. Prasad, M. Pietrzykowski, Soil as a complex ecological system for meeting food and nutritional security, in: Climate Change and Soil Interactions, Elsevier, 2020, pp. 229–269.

[2] C. Jie, C. Jing-zhang, T. Man-zhi, G. Zi-tong, Soil degradation: a global problem endangering sustainable development, J. Geogr. Sci. 12 (2002) 243–252, doi:10.1007/BF02837480.

[3] H. Shayler, M. McBride, E. Harrison, in: Sources and Impacts of Contaminants in Soils, Cornell Waste Management Institute, 2009, p. 6. p.

[4] G.N. Tanjina Hasnat, V. Kumar Singh, R. Singh, E. Lichtfouse, Sources and impacts of emerging contaminants in agroecosystems, in: Sustainable Agriculture Reviews, 50, Springer, Cham, 2021, pp. 3–34.

[5] S. Khan, M. Naushad, E.C. Lima, S. Zhang, S.M. Shaheen, J. Rinklebe, Global soil pollution by toxic elements: current status and future perspectives on the risk assessment and remediation strategies - a review, J. Hazard. Mater. 417 (2021) 126039, doi:10.1016/j.jhazmat.2021.126039.

[6] L.J. Ehlers, R.G. Luthy, Contaminant bioavailability in soil and sediment, Environ. Sci. Technol. 37 (2003) 295–302, doi:10.1021/es03524f.

[7] S. Tajudin, M. Azmi, A. Nabila, Stabilization/solidification remediation method for contaminated soils: a review, IOP Conf. Ser. Mater. Sci. Eng. 136 (2016) 12043, doi:10.1088/1757-899X/136/1/012043.

[8] F.G. Simon, W.W. Müller, Standard and alternative landfill capping design in Germany, Environ. Sci. Policy 7 (2004) 277–290, doi:10.1016/j.envsci.2004.04.002.

[9] in: G. Murtaza, B. Murtaza, N. Niazi, M. Sabir, P. Ahmad, M. Wani, M. Azooz, L.S. Tran, Soil contaminants: sources, effects, and approaches for remediation, in: Improvement of Crops in the Era of Climate Changes, Springer, New York, NY, 2014, pp. 171–196.

[10] P.P. Falciglia, M.G. Giustra, F.G. Vagliasindi, Low-temperature thermal desorption of diesel polluted soils: influence of temperature and soil texture on contaminant removal kinetics, J. Hazard. Mater. 185 (2011) 392–400, doi:10.1016/j.jhazmat.2010.09.046.

[11] G. Dermont, M. Bergeron, G. Mercier, M. Richer-Laflèche, Soil washing for metal removal: a review of physical/chemical technologies and fields of applications, J. Hazard. Mater. 152 (2008) 1–31, doi:10.1016/j.jhazmat.2007.10.043.

[12] J. Pina, J. Merino, A.F. Errazu, V. Bucala, Thermal treatment of soils contaminated with gas oil: influence of soil composition and treatment temperature, J. Hazard. Mater. 94 (2002) 273–290, doi:10.1016/S0304-3894(02)00081-X.

[13] A. Tsitonaki, B. Petri, M. Crimi, H. Mosbaek, R.L. Siegrist, P.L. Bjerg, *In situ* chemical oxidation of contaminated soil and groundwater using persulfate: a review, Crit. Rev. Environ. Sci. Technol. 40 (2010) 55–91, doi:10.1080/10643380802039303.

[14] V. Pande, S.C. Pandey, D. Sati, V. Pande, M. Samant, Bioremediation: an emerging effective approach towards environment restoration, Environ. Sustain. 3 (2020) 91–103, doi:10.1007/s42398-020-00099-w.

[15] I. Gonçalves Sales de Silva, F.C. Gomes de Almeida, N.M. Padilha da Rocha e Silva, A.A. Casazza, A. Converti, L.A. Sarubbo, Soil Bioremediation: overview of technologies and trends, Energies 13 (2020) 4664, doi:10.3390/en13184664.

[16] A. Dzionek, D. Wojcieszynska, U. Guzik, Natural carriers in bioremediation: a review, Electron. J. Biotechnol. 23 (2016) 28–36, doi:10.1016/j.ejbt.2016.07.003.

[17] M.S. El-Geundi, Adsorbents for Industrial Pollution Control, Ads. Sci. Technol. 15 (1997) 777–787, doi:10.1177/026361749701501004.

[18] I. Ali, M. Asim, T.A. Khan, Low cost adsorbents for the removal of organic pollutants from wastewater, J. Environ. Manag. 113 (2012) 170–183, doi:10.1016/j.jenvman.2012.08.028.

[19] A.H. Lahori, Z. Guo, Z. Zhang, R. Li, A. Mahar, M.K. Awasthi, F. Shen, T.A. Sial, F. Kumbhar, P. Wang, S. Jiang, Use of biochar as an amendment for remediation of heavy metal-contaminated soils: prospects and challenges, Pedosphere 27 (2017) 991–1014, doi:10.1016/S1002-0160(17)60490-9.

[20] H. Chaabane, J.-.F. Cooper, L. Azouzi, C.-.M. Coste, Influence of soil properties on the adsorption-desorption of sulcotrione and its hydrolysis metabolites on various soils, J. Agric. Food Chem. 53 (2005) 4091–4095, doi:10.1021/jf040443c.

[21] B.O. Otunola, O.O. Ololade, A review on the application of clay minerals as heavy metal adsorbents for remediation purposes, Environ. Technol. Innov. 18 (2020) 100692, doi:10.1016/j.eti.2020.100692.

[22] M. Guo, W. Song, J. Tian, Biochar-facilitated soil remediation: mechanisms and efficacy variation, Front. Environ. Sci. (2020), doi:10.3389/fen-vs.2020.521512.

[23] S. Deville, Freeze-casting of porous ceramics: a review of current achievements and issues, Adv. Eng. Mater. 10 (2008) 155–169, doi:10.1002/adem.200700270.

[24] S. Deville, E. Saiz, R.K. Nalla, A.P. Tomsia, Freezing as a path to build complex composites, Science 311 (2006) 515–518, doi:10.1126/science.1120937.

[25] Y. Chino, D.C. Dunand, Directionally freeze-cast titanium foam with aligned, elongated pores, Acta Mater. 56 (2008) 105–113, doi:10.1016/j.actamat.2007.09.002.

[26] C. Rieu, C. Parisi, G. Mosser, B. Haye, T. Coradin, F.M. Fernandes, L. Trichet, Topotactic fibrillogenesis of freeze-cast microridged collagen scaffolds for 3D cell culture, ACS Appl. Mater. Interfaces 11 (2019) 14672–14683, doi:10.1021/acsami.9b03219.

[27] G. Shao, D.A.H. Hanaor, X. Shen, A. Gurlo, Freeze casting: from low-dimensional building blocks to aligned porous structures—a review of novel materials, methods, and applications, Adv. Mater. 32 (2020) 1907176, doi:10.1002/adma.201907176.

[28] B.W. Riblett, N.L. Francis, M.A. Wheatley, U.G.K. Wegst, Ice-templated scaffolds with microridged pores direct DRG neurite growth, Adv. Funct. Mater. 22 (2012) 4920–4923, doi:10.1002/adfm.201201323.

[29] K. Qin, C. Parisi, F.M. Fernandes, Recent advances in ice templating: from biomimetic composites to cell culture scaffolds and tissue engineering, J. Mater. Chem. B 9 (2021) 889–907, doi:10.1039/D0TB02506B.

[30] Y. Bai, R. Liu, Y. Wang, H. Xiao, Y. Liu, G. Yuan, High ion transport within a freeze-casted gel film for high-rate integrated flexible supercapacitors, ACS Appl. Mater. Interfaces 11 (2019) 43294–43302, doi:10.1021/acsami.9b16708.

[31] H. Shen, E. Yi, M. Amores, L. Cheng, N. Tamura, D.Y. Parkinson, G. Chen, K. Chen, M. Doeff, Oriented porous LLZO 3D structures obtained by freeze casting for battery applications, J. Mater. Chem. A 7 (2019) 20861–20870, doi:10.1039/C9TA06520B.

[32] M.-.A. Shahbazi, M. Ghalkhani, H. Maleki, Directional freeze-casting: a bioinspired method to assemble multifunctional aligned porous structures for advanced applications, Adv. Eng. Mater. 22 (2020) 200033, doi:10.1002/adem.202000033.

[33] M. Xie, Y. Zhang, M.J. Krasny, C. Bowen, H. Khanbareh, N. Gathercole, Flexible and active self-powered pressure, shear sensors based on freeze-casting ceramic-polymer composites, Energy Environ. Sci. 11 (2018) 29192927, doi:10.1039/C8EE01551A.

[34] D. Mohnen, Pectin structure and biosynthesis, Curr. Opin. Plant Biol. 11 (2008) 266–277, doi:10.1016/j.pbi.2008.03.006.

[35] G. Carturan, R. Dal Toso, S. Boninsegna, R. Dal Monte, Encapsulation of functional cells by sol-gel silica: actual progress and perspectives for cell therapy, J. Mater. Chem. 14 (2004) 2087–2098, doi:10.1039/B401450B.

[36] H.P. van Dokkum, J.H.J. Hulskotte, K.J.M. Kramer, J. Wilmot, Emission, fate and effects of soluble silicates (waterglass) in the aquatic environment, Environ. Sci. Technol. 38 (2004) 515–521, doi:10.1021/es0264697.

[37] S. Christoph, A. Hamraoui, E. Bonnin, C. Garnier, T. Coradin, F.M. Fernandes, Ice-tempating beet-root pectin foams: controlling texture, mechanics and capillary properties, Chem. Eng. J. 350 (2018) 20–28, doi:10.1016/j.cej.2018.05.160.

[38] S. Christoph, J. Kwiatoszynski, T. Coradin, F.M. Fernandes, Cellularized cellular solids via freeze-casting, Macromol. Biosci. 16 (2016) 182–187, doi:10.1002/mabi.201500319.

[39] M.F. Ashby, On the engineering properties of materials, Acta Metall. 37 (1989) 1273–1293, doi:10.1016/0001-6160(89)90158-2.

[40] T. Yoshimura, K. Sengoku, R. Fujioka, Pectin-based surperabsorbent hydrogels crosslinked by some chemicals: synthesis and characterization, Polym. Bull. 55 (2005) 123–129, doi:10.1007/s00289-005-0422-1.

[41] A. Gendron-Badou, T. Coradin, J. Maquet, F. Frölich, J. Livage, Spectroscopic characterization of biogenic silica, J. Non-Cryst. Solids 316 (2003) 331–337, doi:10.1016/S0022-3093(02)01634-4.

[42] Z. Püspöki, M. Storath, D. Sage, M. Unser, Transforms and operators for directional bioimage analysis: a survey, Adv. Anat. Embryol. Cell Biol. 219 (2016) 69–93, doi:10.1007/978-3-319-28549-8_3.

[43] C. Cameselle, S. Gouveia, A. Cabo, M.A. Rodrigo, E.V. Dos Santos, Electrokinetic soil flushing, in: Electrochemically Assisted Remediation of Contaminated Soils, Springer, 2021, pp. 111–132.